AJNR

Different Patterns of Fornix Damage in Idiopathic Normal Pressure Hydrocephalus and Alzheimer Disease

T. Hattori, R. Sato, S. Aoki, T. Yuasa and H. Mizusawa

AJNR Am J Neuroradiol 2012, 33 (2) 274-279
doi: https://doi.org/10.3174/ajnr.A2780
http://www.ajnr.org/content/33/2/274

ORIGINAL RESEARCH

Different Patterns of Fornix Damage in Idiopathic Normal Pressure Hydrocephalus and Alzheimer Disease

T. Hattori
R. Sato
S. Aoki
T. Yuasa
H. Mizusawa

BACKGROUND AND PURPOSE: The fornix contains efferent fibers of the hippocampus and is in close contact with the corpus callosum. Part of the fornix is directly attached to the corpus callosum, and another part is suspended from the corpus callosum via the septum pellucidum. DTI can be used to evaluate the morphology and microstructural integrity of the fornix. We examined the pattern of fornix damage in patients with iNPH or AD.

MATERIALS AND METHODS: We enrolled 22 patients with iNPH, 20 with AD, and 20 healthy controls. DTI data were obtained. The morphology (volume, length, and mean cross-sectional area) and FA values of the fornix were evaluated by using tract-specific analysis and compared among groups.

RESULTS: The volume, cross-sectional area, and FA value of the fornix were significantly smaller in patients with iNPH than in controls, whereas the length was significantly greater. In patients with AD, the volume, mean cross-sectional area, and FA value of the fornix were significantly smaller than those in controls, whereas the length was not altered. The fornix was significantly longer in patients with iNPH than in patients with AD, whereas the volume and cross-sectional areas were significantly smaller.

CONCLUSIONS: Our results suggest that the different pathogeneses of these diseases lead to fornix damage through different mechanisms: through mechanical stretching due to lateral ventricular enlargement and corpus callosum deformation in patients with iNPH, and through degeneration secondary to hippocampal atrophy in patients with AD.

ABBREVIATIONS: AD = Alzheimer disease; FA = fractional anisotropy; iNPH = idiopathic normal-pressure hydrocephalus; MMSE = Mini-Mental State Examination

The fornix is composed mainly of the efferent fibers of the hippocampus.[1] Anatomically, part of the fornix is directly attached to the splenium and posterior body of the corpus callosum, and another part is suspended from the corpus callosum via the septum pellucidum.[2] Thus, the fornix may be susceptible to both atrophy of the hippocampus and the mechanical pressure that is applied if the corpus callosum is deformed.

Patients with iNPH have enlarged lateral ventricles.[3] The corpus callosum is deformed upwardly in these patients, resulting in stretching and thinning,[4,5] primarily due to mechanical pressure from the enlarged lateral ventricles[6]; this may also affect the fornix. AD results primarily in severe degeneration of the hippocampus,[7] which can result in secondary degeneration of the efferent fibers of the hippocampus, including the fornix.[8,9] Therefore, we hypothesized that the different pathogeneses of iNPH and AD cause different patterns of fornix damage.

DTI has been used in vivo to quantitatively evaluate changes in white matter due to various neurodegenerative diseases.[10,11] Tract-specific analysis, 1 method of DTI data analysis, uses diffusion tensor tractography to pinpoint anatomic landmarks, and it can be used to quantitatively evaluate the morphology and microstructural integrity of target tracts,[12-14] including the fornix.[15] To date, to our knowledge, no studies have investigated the features of the fornix in patients with iNPH or AD by using tract-specific analysis.

Here, we aimed to elucidate the patterns of fornix damage in patients with iNPH or AD by using DTI.

Materials and Methods

Subject Selection

Subjects were consecutively recruited from among patients who visited the department of neurology or neurosurgery at Kamagaya General Hospital in Chiba, Japan, from April 2009 to February 2011. All subjects were medically interviewed and were given general and neurologic examinations, including the MMSE, by neurologists (T.H. and T.Y.). Information on reports of memory loss or other subjective cognitive deficits was gathered by means of a caregiver-based interview for all patients. We enrolled patients with probable iNPH according to the clinical diagnostic criteria of iNPH.[3] To further classify the enrolled patients with iNPH, we also used the Japanese clinical guidelines for iNPH.[16] Possible iNPH was diagnosed on the basis of clinical history, brain imaging, physical findings, and physiologic findings. Probable iNPH was diagnosed if symptomatic improvement was confirmed after spinal tap test in a patient with possible iNPH. Definite iNPH was diagnosed if symptomatic improvement was confirmed after a shunt operation in a patient with probable iNPH. We also enrolled patients with probable AD according to the clinical diagnostic criteria of AD.[17] Healthy control subjects were selected on

Received May 11, 2011; accepted after revision July 13.

From the Department of Neurology and Neurological Sciences (T.H., H.M.), Graduate School, Tokyo Medical and Dental University, Tokyo, Japan; Department of Radiology (T.H., S.A., R.S.), Juntendo University, Tokyo, Japan; Department of Neurology (T.H., T.Y.), Kamagaya General Hospital, Chiba, Japan; Department of Neurology (T.H.), Kanto Central Hospital, Tokyo, Japan; and Department of Radiological Sciences and Graduate School of Human Health Sciences (R.S.), Tokyo Metropolitan University, Tokyo, Japan.

Please address correspondence to Takaaki Hattori, MD, PhD, Department of Neurology, Kanto Central Hospital, 6–25-1, Kamiyoga, Setagaya-ku, Tokyo, 158-8531, Japan; e-mail: takaaki-hattori@umin.ac.jp

http://dx.doi.org/10.3174/ajnr.A2780

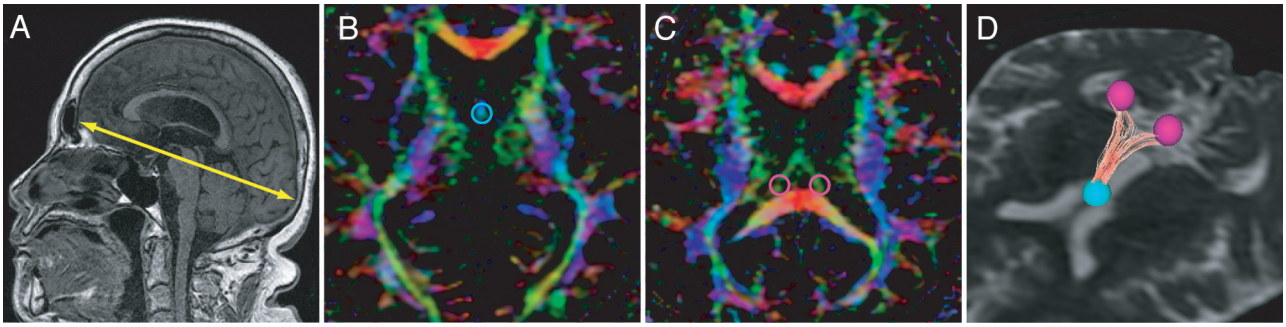

Fig 1. Tractography of the fornix by using tract-specific analysis. *A,* The maximal anteroposterior length of the inner skull on the parallel line with the anterior/posterior commissure line is measured on the midline sagittal plane by using 3D T1-weighted images. *B* and *C,* Diffusion tensor tractography of the fornix is generated by using the seed region of interest (*B*) on the convergence of the 2 columns in the body of the fornix and the target regions of interest (*C*) on the right or the left crus of the fornix in front of the corpus callosum. *D,* An example of the drawn tractography of the fornix of a healthy subject.

the basis of a normal result on the MMSE and normal neurologic examination findings.

Subjects with focal brain lesions or white matter abnormalities outside the normal range were identified by reviewing axial fluid-attenuated inversion recovery scans of each subject; these patients were excluded, as were patients with images that showed motion artifacts. Subjects who had other brain disorders or underlying diseases that could affect the brain, such as uncontrolled hypertension or chronic kidney disease, were also excluded.

This study was approved by the institutional review board of Kamagaya General Hospital, Japan, and written informed consent was obtained from all subjects.

MR Imaging Data Acquisition

MR imaging data were obtained with a 1.5T clinical scanner (Signa Excite; GE Healthcare, Milwaukee, Wisconsin). Fluid-attenuated inversion recovery images were obtained with fast spin-echo imaging (TR = 12 000 ms, TE = 106 ms, FOV = 220 mm, matrix = 512 × 512, flip angle = 90°, section thickness = 6 mm, 20 sections, intersection gaps = 1 mm). 3D T1-weighted sagittal images were obtained with 3D spoiled gradient-echo imaging (TR = 5.5 ms, TE = 1.4 ms, FOV = 220 mm, matrix = 256 × 256, flip angle = 20°, section thickness = 1.5 mm, 116 sections; no intersection gaps). DTI data were obtained with a single-shot echo-planar sequence (TR = 14 000 ms, TE = 103.5 ms, b=1,000 s/mm^2, 13 directions of motion-probing gradients, FOV = 280 mm, matrix = 128 × 128 [interpolated image matrix size, 256 × 256], section thickness = 3 mm, averaging = 2, number of sections = 50; no intersection gaps; total acquisition time = 6 minutes 32 seconds).

Data Analysis

The maximal anteroposterior length of the inner skull on the line parallel to the anterior/posterior commissure line was measured on the midline sagittal plane by using 3D T1-weighted images (Fig 1*A*).

DTI data were analyzed by using dTV II and Volume-One 1.72 software developed by Masutani et al (http://www.ut-radiology.umin.jp/people/masutani/dTV.htm) and running on Windows XP Professional (Microsoft, Redmond, Washington), which were frequently used in previous studies.[12,13,15] The threshold of line-tracking was set as an FA value of >.05 because this was the optimal condition to stably draw the tractography of the fornix. Diffusion tensor tractography of the fornix was generated by using a 2-regions-of-interest method: A seed region of interest (sphere, 3 mm in diameter; Fig 1*B*) was placed on the convergence of the 2 columns in the body of the fornix, and the target regions of interest (spheres, 5 mm in diameter; Fig 1*C*) were placed on the right and left crura of the fornix anterior to the corpus callosum on the axial plane of the color-coded FA map. In the color-coded FA maps, the orientation of the axial eigenvector was color-coded per voxel according to the red-green-blue convention, red indicating a predominant left-right orientation within each voxel, green indicating an anteroposterior orientation, and blue indicating a superior-inferior orientation.

Voxelization of the tractography of the fornix was performed from a seed region of interest to the target regions of interest (Fig 2*B*, -*E*, -*H*), in accordance with the method used in a previous study.[15] In our study, the "volume" of the fornix was defined as the total volume of voxels included in the voxelized tractography of the fornix. The length of fornix between the seed region of interest and the target region of interest was also measured by using dTV. The length index of the fornix was calculated by dividing the length of the fornix by the maximal anteroposterior length of the inner skull. The mean cross-sectional area of the fornix was measured by dividing the volume of the fornix by the length of the fornix. Shape processing (voxels were dilated once and eroded twice) was performed for the drawn tractography of the fornix to obtain the tract skeleton, excluding the outer voxels that also contained nonfiber structures and avoiding the partial volume effects (Fig 2*C*, -*F*, -*I*).[15] The FA value was measured in the voxelized tractography of the fornix after shape processing. When analyzing data, the operator (R.S.) was blinded to the clinical information of each subject to avoid bias.

Statistical Analysis

Statistical analysis among groups was performed by using ANOVA with a post hoc Tukey Honestly Significant Difference test for continuous variables, the Kruskal-Wallis test with post hoc Mann-Whitney U tests for noncontinuous variables, and the χ^2 test for categoric data. The criterion of statistical significance was $P < .05$.

Analyses were performed with the Statistical Package for Social Sciences, Version 11 (SPSS Inc, Chicago, Illinois). The results are expressed as means ± SD.

Results

Demographic and Clinical Features

We enrolled 22 patients with iNPH, 20 with AD, and 20 age- and sex-matched control subjects (Table). All patients with iNPH showed gait disturbance and a varying degree of cognitive dysfunction and incontinence. All patients with iNPH had

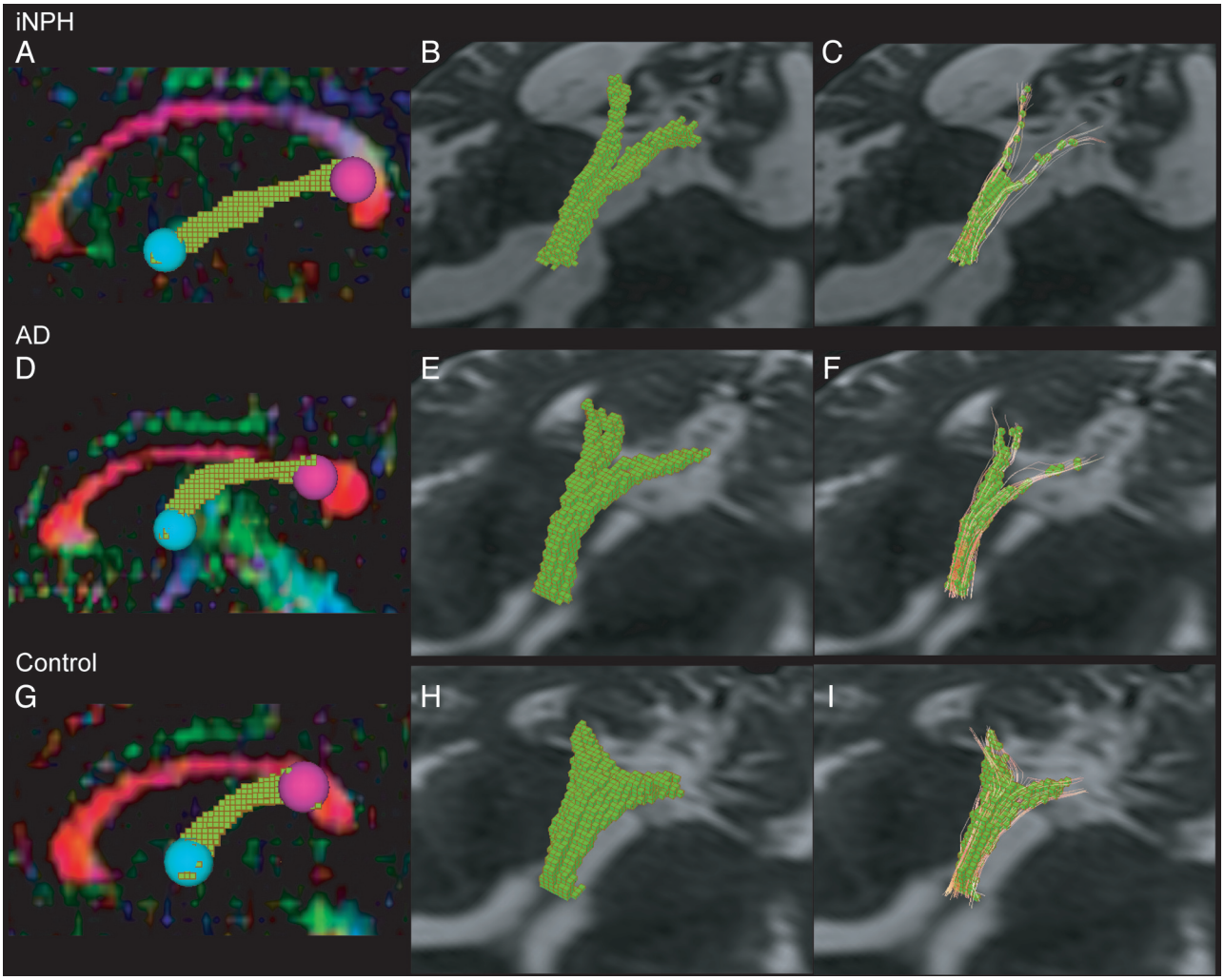

Fig 2. Voxelization of the tractography of the fornix. The voxelized tractography of the fornix on the sagittal plane of the color-coded FA map is shown (*A, D, G*). The morphologic features are evaluated by using the voxelized tractography of the fornix (*B, E, H*). The diffusion tensor metrics are evaluated in the voxelized tractography of the fornix after shape-processing (*C, F, I*). The tractography for iNPH (*A, B, C*), AD (*D, E, F*), and controls (*G, H, I*) are shown.

Demographic and clinical data of patients with iNPH or AD and control subjects[a]

	A	B	C		
Characteristics	iNPH (n = 22)	AD (n = 20)	Controls (n = 20)	P Value	Post Hoc Significance
Age (yr)	77.3 ± 4.9	74.6 ± 5.7	73.9 ± 6.0	.622	
Male/female	10:12	10:10	7:13	.617	
MMSE score	22.1 ± 3.7	18.3 ± 6.7	28.6 ± 0.0	<.001	A, B < C[b]
Evans' index	0.36 ± 0.05	0.29 ± 0.03	0.27 ± 0.03	<.001	A > B, C[b]
Vascular risk factors					
Hypertension (%)	27.8	36.4	42.11	.561	
Diabetes mellitus (%)	16.7	18.2	0	.157	
Dyslipidemia (%)	22.2	27.3	0	.168	

[a] Data are shown as mean ± SD.
[b] $P < .001$.

communicating hydrocephalus (Evans' index >0.3) and narrowed CSF spaces with high convexity on MR imaging. A spinal tap test was performed, and symptomatic improvement was confirmed in all patients. A shunt operation was performed, and symptomatic improvement was confirmed in 12 patients with iNPH. A shunt operation was not performed for 10 patients with iNPH. The enrolled patients with iNPH fulfilled the Japanese diagnostic criteria[16] of probable iNPH (n = 10) or definite iNPH (n = 12). The Evans' index was significantly higher in patients with iNPH than in other subjects ($P < .001$). Patient groups had significantly lower MMSE scores than control subjects ($P < .001$). There were no significant differences in age, sex, or vascular risk factors (hypertension, diabetes mellitus, or dyslipidemia) among the groups.

Morphologic Features of the Fornix

Examples of tractography of the fornix in patients with iNPH or AD and control subjects are shown in Fig 2. The tractogra-

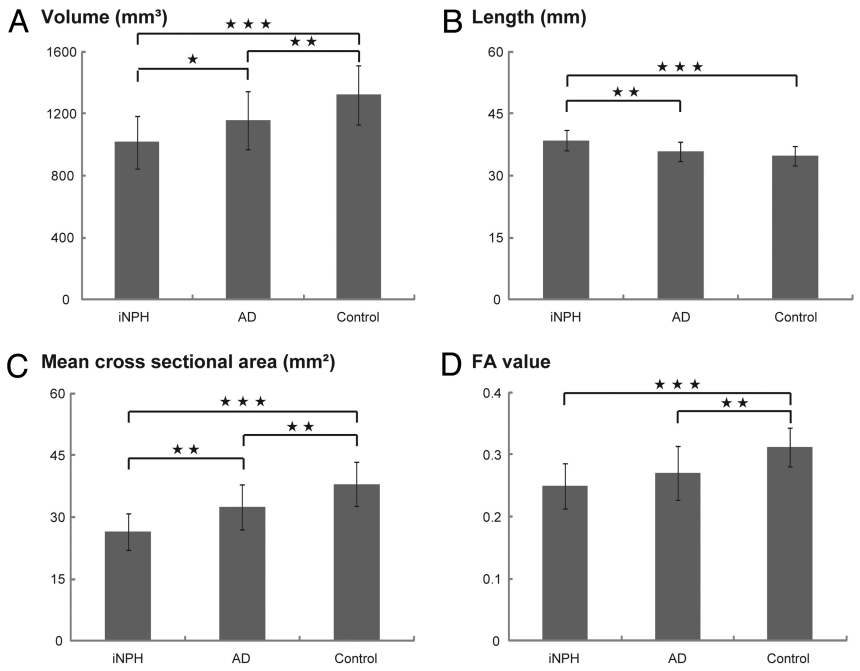

Fig 3. Comparison of morphologic features and FA value of the fornix. The volume (*A*), length (*B*), mean cross-sectional area (*C*), and FA value (*D*) of the fornix are shown. The asterisk indicates $P < .05$; double asterisks, $P < .01$; triple asterisks, $P < .001$.

phy showed that the fornix was stretched in the anteroposterior direction in patients with iNPH compared with that of patients with AD and control subjects (Fig 2*A*, -*D*, -*G*). The diameter of the fornix was smaller in patients with iNPH than in patients with AD or controls and smaller in patients with AD than in controls (Fig 2*A*, -*D*, -*G*). The volume of the fornix was smaller in patients with iNPH or AD than in control subjects (Fig 2*B*, -*E*, -*H*).

The maximal anteroposterior length of the inner skull did not differ significantly among the 3 groups (iNPH: 158 ± 5.5 mm; AD: 157 ± 7.1 mm; control: 156 ± 7.6 mm; ANOVA $P = .664$). The volume of the fornix was significantly smaller in patients with iNPH than in patients with AD ($P = .036$) or control subjects ($P < .001$); the volume was also smaller in patients with AD than in control subjects ($P = .009$) (Fig 3*A*). The length and length index (iNPH: 0.32 ± 0.03; AD: 0.30 ± 0.02; control: 0.29 ± 0.02; ANOVA $P = .004$) of the fornix were significantly greater in patients with iNPH than in patients with AD ($P = .001$, $P = .024$, respectively) or control subjects ($P < .001$, $P = .006$, respectively) (Fig 3*B*). The mean cross-sectional area of the fornix, including bilateral parts of the fornix from the crus to the column, was significantly smaller in patients with iNPH than in patients with AD ($P = .001$) or control subjects ($P < .001$) and was significantly smaller in patients with AD than in control subjects ($P = .002$) (Fig 3*C*).

Integrity of the Fornix: FA Values

The mean FA values of the fornix measured by using tract-specific analysis are shown in Fig 3*D*. The FA values were significantly lower in patients with iNPH ($P < .001$) and patients with AD ($P = .002$) than in control subjects.

Discussion

This is the first DTI study to evaluate the morphology and microstructural integrity of the fornix in patients with iNPH or AD and control subjects by using tract-specific analysis. We evaluated the FA value on the basis of the assumption that the FA value reflects the microstructural integrity of the fornix.[18,19] Our results showed different patterns of fornix damage in patients with iNPH and AD. We propose that the different pathogeneses of iNPH and AD caused these different patterns of fornix damage.

In patients with iNPH, the corpus callosum is elevated and stretched in the anteroposterior direction by the mechanical pressure from the enlarged lateral ventricles.[4,5] Part of the fornix is directly attached to the splenium and posterior body of the corpus callosum, and another part of the fornix is suspended from the corpus callosum via the septum pellucidum.[2] In addition, the crura of the fornix are fixed to the floor of the lateral ventricle (ie, the medial edge of the hippocampus) and connect to the fimbria. Thus, in patients with iNPH, the fornix may be stretched in the anteroposterior direction with or without stretching in the superior-inferior direction by the deformed corpus callosum. These complex mechanical pressures may alter the morphology and integrity of the fornix in patients with iNPH. Our study showed that the volume and the mean cross-sectional area of the fornix were significantly lower and the length of the fornix was higher in patients with iNPH than in controls. In addition, the FA value of the fornix was significantly lower in patients with iNPH than in controls. The decreased FA value indicates the decreased microstructural integrity of the fornix, possibly reflecting the multiple pathologies such as axonal loss, demyelination, interstitial edema, and/or reactive gliosis.[20-22] These results support the hypothesis that in patients with iNPH, the fornix is damaged

by mechanical pressure from the enlarged lateral ventricle via the deformed corpus callosum, resulting in atrophy, thinning, and elongation, with decreased microstructural integrity.

In patients with AD, the hippocampus is the primary site of damage and degenerates severely.[7] The fornix is composed mainly of the efferent fibers of the hippocampus. Thus, the fornix can undergo secondary degeneration due to hippocampal atrophy in patients with AD.[23] Our results showed that the volume and mean cross-sectional area of the fornix were significantly lower in patients with AD than in controls, whereas the length of the fornix was not altered. Atrophy of the fornix in patients with AD was also shown in previous volumetric studies.[8,9] In addition, the FA value was significantly lower in patients with AD than in controls; this result is also consistent with those of previous DTI studies.[23-26] These results support the hypothesis that in patients with AD, the fornix degenerates secondary to the hippocampal atrophy, resulting in atrophy and thinning but not elongation, with decreased microstructural integrity.

The hippocampus may also be damaged in patients with iNPH, possibly because of AD-type pathology (which has been reported in biopsy samples of the cortex[27]) or metabolic derangement.[28] One previous DTI study showed that the FA value in the hippocampus was significantly lower in patients with iNPH than in control subjects but significantly higher in patients with iNPH than in patients with AD.[29] These results suggest that patients with iNPH may also have hippocampal damage, though milder than that in patients with AD. Our results show that another pathogenesis—most likely mechanical pressure—is necessary to cause the significantly more atrophied, thinned, and elongated morphology of the fornix compared with that in patients with AD.

One of the characteristic MR imaging findings of patients with iNPH is the small callosal angle. The callosal angle is defined as the angle between the right and left interhemispheric fibers that form the corpus callosum, and it is a promising tool to successfully differentiate patients with iNPH from others.[30] However, the mechanism leading to the small callosal angle in patients with iNPH has not yet been elucidated. Because the fornix is in close contact with the corpus callosum, we consider that the right and left interhemispheric fibers are elevated by the mechanical pressure from the enlarged lateral ventricles, whereas the corpus callosum is restrained to the floor of the lateral ventricle via the fornix, resulting in the small callosal angle. In other words, a small callosal angle in patients with iNPH may indicate the presence of mechanical pressure and resulting mechanical damage to the fornix.

The fornix connects the hippocampus and the mamillary body and plays a pivotal role in learning and memory.[2] In fact, fornix infarction causes memory impairments such as anterograde and retrograde amnesia.[31] Although patients with iNPH have various cognitive deficits, such as memory impairment, executive dysfunction, and visuospatial dysfunction[32,33] that might be attributed to several different substrates, the memory impairment may be, at least in part, caused by the fornix damage. Future studies that specifically evaluate memory function in patients with iNPH and investigate its correlation with DTI findings are needed.

This study, however, had limitations. First, only limited information on the pathology of iNPH, especially in regard to the fornix, is available, and the pathologic basis for the altered morphology and integrity of the fornix should be the subject of a future study. Second, we did not evaluate DTI in patients with iNPH who had undergone shunt surgery. We, therefore, do not know whether shunt surgery is capable of reversing these changes in patients with iNPH.

Conclusions

This study is the first to evaluate the morphology and microstructural integrity of the fornix in patients with iNPH or AD by using DTI. Our results suggest that the fornix is damaged through different means in patients with iNPH and AD. DTI analysis of the fornix may be a promising tool to differentiate patients with iNPH from patients with AD or control subjects and may elucidate parts of the substrate for various cognitive deficits in patients with iNPH.

Acknowledgments

We thank Yu Takeuchi, MD, of the department of neurology, and Hiroaki Sawaura, MD, of the department of neurosurgery, at Kamagaya General hospital for their cooperation. We also thank the Comprehensive Brain Science Network of the Ministry of Education, Culture, Sports, Science and Technology for providing us with a good environment for our discussions.

Disclosures: Shigeki Aoki—*RELATED: Grant/Fees for Participation in Review Activities Such as Data Monitoring Boards, Statistical Analysis, End Point Committees, and the Like*: Ministry of Education, Science, Sports and Culture of Japan, Comments: Grant-in-Aid for scientific research in innovative areas (Comprehensive Brain Science Network); *UNRELATED: Grants/Grants Pending*: Ministry of Education, Science, Sports and Culture of Japan, Comments: Grant-in-Aid for scientific research in innovative areas (Comprehensive Brain Science Network). Hidehiro Mizusawa—*UNRELATED: Board Membership: Shinkei*, Igakushoin Co, *Clinical Neuroscience*, Chugai Igaku Co; *Grants/Grants Pending*: research grant;* *Payment for Lectures, Including Service on Speakers Bureaus*: Tonabe mitsubishi, Sanofi-Aventis, Comments: honoraria for sponsored lectures. *Money paid to institution.

References

1. Cassel JC, Duconseille E, Jeltsch H, et al. **The fimbria-fornix/cingular bundle pathways: a review of neurochemical and behavioural approaches using lesions and transplantation techniques.** *Prog Neurobiol* 1997;51:663–716
2. Griffiths PD, Batty R, Reeves MJ, et al. **Imaging the corpus callosum, septum pellucidum and fornix in children: normal anatomy and variations of normality.** *Neuroradiology* 2009;51:337–45
3. Relkin N, Marmarou A, Klinge P, et al. **Diagnosing idiopathic normal-pressure hydrocephalus.** *Neurosurgery* 2005;57:S4–16, discussion ii-v
4. Roricht S, Meyer BU, Woiciechowsky C, et al. **Callosal and corticospinal tract function in patients with hydrocephalus: a morphometric and transcranial magnetic stimulation study.** *J Neurol* 1998;245:280–88
5. Mataro M, Matarin M, Poca MA, et al. **Functional and magnetic resonance imaging correlates of corpus callosum in normal pressure hydrocephalus before and after shunting.** *J Neurol Neurosurg Psychiatry* 2007;78:395–98
6. Gammal TE, Allen MB Jr, Brooks BS, et al. **MR evaluation of hydrocephalus.** *AJR Am J Roentgenol* 1987;149:807–13
7. Braak H, Alafuzoff I, Arzberger T, et al. **Staging of Alzheimer disease-associated neurofibrillary pathology using paraffin sections and immunocytochemistry.** *Acta Neuropathol* 2006;112:389–404. Epub 2006 Aug 12
8. Copenhaver BR, Rabin LA, Saykin AJ, et al. **The fornix and mammillary bodies in older adults with Alzheimer's disease, mild cognitive impairment, and cognitive complaints: a volumetric MRI study.** *Psychiatry Res* 2006;147:93–103
9. Callen DJ, Black SE, Gao F, et al. **Beyond the hippocampus: MRI volumetry confirms widespread limbic atrophy in AD.** *Neurology* 2001;57:1669–74
10. Sage CA, Peeters RR, Gorner A, et al. **Quantitative diffusion tensor imaging in amyotrophic lateral sclerosis.** *Neuroimage* 2007;34:486–99
11. Hattori T, Orimo S, Aoki S, et al. **Cognitive status correlates with white matter alteration in Parkinson's disease.** *Hum Brain Mapp* 2011 Apr 14. [Epub ahead of print]
12. Taoka T, Kin T, Nakagawa H, et al. **Diffusivity and diffusion anisotropy of**

cerebellar peduncles in cases of spinocerebellar degenerative disease. *Neuroimage* 2007;37:387–93
13. Aoki S, Iwata NK, Masutani Y, et al. **Quantitative evaluation of the pyramidal tract segmented by diffusion tensor tractography: feasibility study in patients with amyotrophic lateral sclerosis.** *Radiat Med* 2005;23:195–99
14. Hattori T, Yuasa T, Aoki S, et al. **Altered microstructure in corticospinal tract in idiopathic normal pressure hydrocephalus: Alzheimer disease and Parkinson disease with dementia.** *AJNR Am J Neuroradiol* 2011;32:1681–87
15. Yasmin H, Aoki S, Abe O, et al. **Tract-specific analysis of white matter pathways in healthy subjects: a pilot study using diffusion tensor MRI.** *Neuroradiology* 2009;51:831–40
16. Ishikawa M and the Guideline Committee for Idiopathic Normal Pressure Hydrocephalus, Japanese Society of Normal Pressure Hydrocephalus. **Clinical guidelines for idiopathic normal pressure hydrocephalus.** *Neurol Med Chir (Tokyo)* 2004;44:222–23
17. McKhann GM, Knopman DS, Chertkow H, et al. **The diagnosis of dementia due to Alzheimer's disease: recommendations from the National Institute on Aging-Alzheimer's Association workgroups on diagnostic guidelines for Alzheimer's disease.** *Alzheimers Dement* 2011;7:263–69
18. Dineen RA, Vilisaar J, Hlinka J, et al. **Disconnection as a mechanism for cognitive dysfunction in multiple sclerosis.** *Brain* 2009;132:239–49
19. Sage CA, Van Hecke W, Peeters R, et al. **Quantitative diffusion tensor imaging in amyotrophic lateral sclerosis: revisited.** *Hum Brain Mapp* 2009;30:3657–75
20. Nucifora PG, Verma R, Lee SK, et al. **Diffusion-tensor MR imaging and tractography: exploring brain microstructure and connectivity.** *Radiology* 2007;245:367–84
21. Concha L, Livy DJ, Beaulieu C, et al. **In vivo diffusion tensor imaging and histopathology of the fimbria-fornix in temporal lobe epilepsy.** *J Neurosci* 2010;30:996–1002
22. van Eijsden P, Otte WM, van der Hel WS, et al. **In vivo diffusion tensor imaging and ex vivo histologic characterization of white matter pathology in a post-status epilepticus model of temporal lobe epilepsy.** *Epilepsia* 2011;52:841–45. Epub 2011 Mar 2
23. Agosta F, Pievani M, Sala S, et al. **White matter damage in Alzheimer disease and its relationship to gray matter atrophy.** *Radiology* 2010;258:853–63
24. Kantarci K, Avula R, Senjem ML, et al. **Dementia with Lewy bodies and Alzheimer disease: neurodegenerative patterns characterized by DTI.** *Neurology* 2010;74:1814–21
25. Pievani M, Agosta F, Pagani E, et al. **Assessment of white matter tract damage in mild cognitive impairment and Alzheimer's disease.** *Hum Brain Mapp* 2010;31:1862–75
26. Liu Y, Spulber G, Lehtimaki KK, et al. **Diffusion tensor imaging and tract-based spatial statistics in Alzheimer's disease and mild cognitive impairment.** *Neurobiol Aging* 2011;32:1558–71. Epub 2009 Nov 12
27. Del Bigio MR, Cardoso ER, Halliday WC. **Neuropathological changes in chronic adult hydrocephalus: cortical biopsies and autopsy findings.** *Can J Neurol Sci* 1997;24:121–26
28. Kondziella D, Sonnewald U, Tullberg M, et al. **Brain metabolism in adult chronic hydrocephalus.** *J Neurochem* 2008;106:1515–24
29. Hong YJ, Yoon B, Shim YS, et al. **Differences in microstructural alterations of the hippocampus in Alzheimer disease and idiopathic normal pressure hydrocephalus: a diffusion tensor imaging study.** *AJNR Am J Neuroradiol* 2010;31:1867–72
30. Ishii K, Kanda T, Harada A, et al. **Clinical impact of the callosal angle in the diagnosis of idiopathic normal pressure hydrocephalus.** *Eur Radiol* 2008;18:2678–83
31. Korematsu K, Hori T, Morioka M, et al. **Memory impairment due to a small unilateral infarction of the fornix.** *Clin Neurol Neurosurg* 2010;112:164–66
32. Iddon JL, Pickard JD, Cross JJ, et al. **Specific patterns of cognitive impairment in patients with idiopathic normal pressure hydrocephalus and Alzheimer's disease: a pilot study.** *J Neurol Neurosurg Psychiatry* 1999;67:723–32
33. Devito EE, Pickard JD, Salmond CH, et al. **The neuropsychology of normal pressure hydrocephalus (NPH).** *Br J Neurosurg* 2005;217–24